Engineering Structures 323 (2025) 119310

Contents lists available at ScienceDirect

Engineering Structures

journal homepage: www.elsevier.com/locate/engstruct

Cyclic behavior of beam-to-upright bolted connections: Experimental study of Chilean steel storage racks

Eduardo Nuñez [a,*], Ramón Mata [b], Marcelo Sanhueza [a], Matías Hernández [a], Nelson Maureira [a], Néstor Guerrero [c]

[a] Department of Civil Engineering, Universidad Católica de La Santísima Concepción, Concepción, Chile
[b] Facultad de Ingeniería, Arquitectura y Diseño, Universidad San Sebastián, Lientur, 1457 Concepción, Chile
[c] Department of Civil Engineering, Universidad de Ibagué, Tolima, Colombia

ARTICLE INFO

Keywords:
Steel racks
Cold formed
Cyclic behavior
Experimental research
Bolt pretension

ABSTRACT

In this research an experimental study to assess the cyclic behavior of bolted moment connection in racks structures is performed. The effect of bolt pretension in the response is evaluated. Sixteen full-scale steel rack joint configurations were subjected to cyclic load according to the protocol established in AISC Seismic provisions. The cyclic performance was evaluated in terms of hysteretic response, failure mechanism, energy dissipation, stiffness, and rotation on the components. Two different configurations were studied. The results showed that the steel rack connections using a 70 % of bolt pretension can accommodate a 0.8 My at 0.04 rad of drift angle, while the joints without bolt pretension reached values below 0.7 My at 4 % of rotation. The failure mechanism was controlled by weld fracture at 4 % of the rotation. A high dispersion in the energy dissipation pattern was obtained and a drop in energy dissipation of up to 4 times in all specimens tested for a 4 % rotation was developed. This phenomenon is due to the welding rupture between the beam and the L-connector. A degradation of the secant stiffness reached up to 60 % for 2 % rotation. Finally, the most important effect of bolt pretension on the cyclic response of steel rack connections was achieved in the increase of flexural resistance and rotation developed.

1. Introduction

Nowadays, the steel storage racks are an important part of the supply chain in companies providing products to the market. Nevertheless, from a structural point of view, racks are steel structures with sections generally manufactured from cold-formed steel sections with limited capacity to resist local buckling. In addition, their structural configuration would be similar to moment frames in down-aisle direction and braced frames in cross-aisle direction, however, their limited stiffness, high global slenderness and highly deformable connections completely differentiate them from traditional systems, requiring their design to be specific and with their own characteristics.

In general, steel racks subjected to gravity loads have an acceptable behavior, while to resist lateral forces such as the seismic forces, have shown a limited performance that has motivated the study of their global behavior and their connections. Several investigations have been conducted, which have allowed improving their performance. Despite the progress achieved, new research is required to improve the performance of racks structures and their connections. For this reason, research addressing this topic is discussed as follow. To provide ductility for rack connections, the study by Godley et al. [1] evaluated the deformation capacity in braced and unbraced racks. The results showed that the required ductility is independent of the connector stiffness. In addition, the connector stiffness provides different ductility levels and proposes a method of defining ductility requirements of the beam to column connection.

An experimental study conducted by Aguirre et al. [2] to assess the seismic behavior of racks structures was performed. Static and cyclic loads were applied to racks connections. The results showed that the failure mode is initiated with yielding of hooks and the hysteresis curve reached high levels of pinching. Bajoria et al. [3] studied the flexibility of beam-to-column connectors using the conventional cantilever experimental method. On the other hand, global studies were performed by Sarawit et al. [4] and Bajoria et al. [5]. The results showed that the notional load method is recommended to design steel racks and simplified models can be used to design the storage racks.

* Corresponding author.
E-mail address: enunez@ucsc.cl (E. Nuñez).

https://doi.org/10.1016/j.engstruct.2024.119310
Received 14 June 2024; Received in revised form 9 October 2024; Accepted 8 November 2024
Available online 13 November 2024

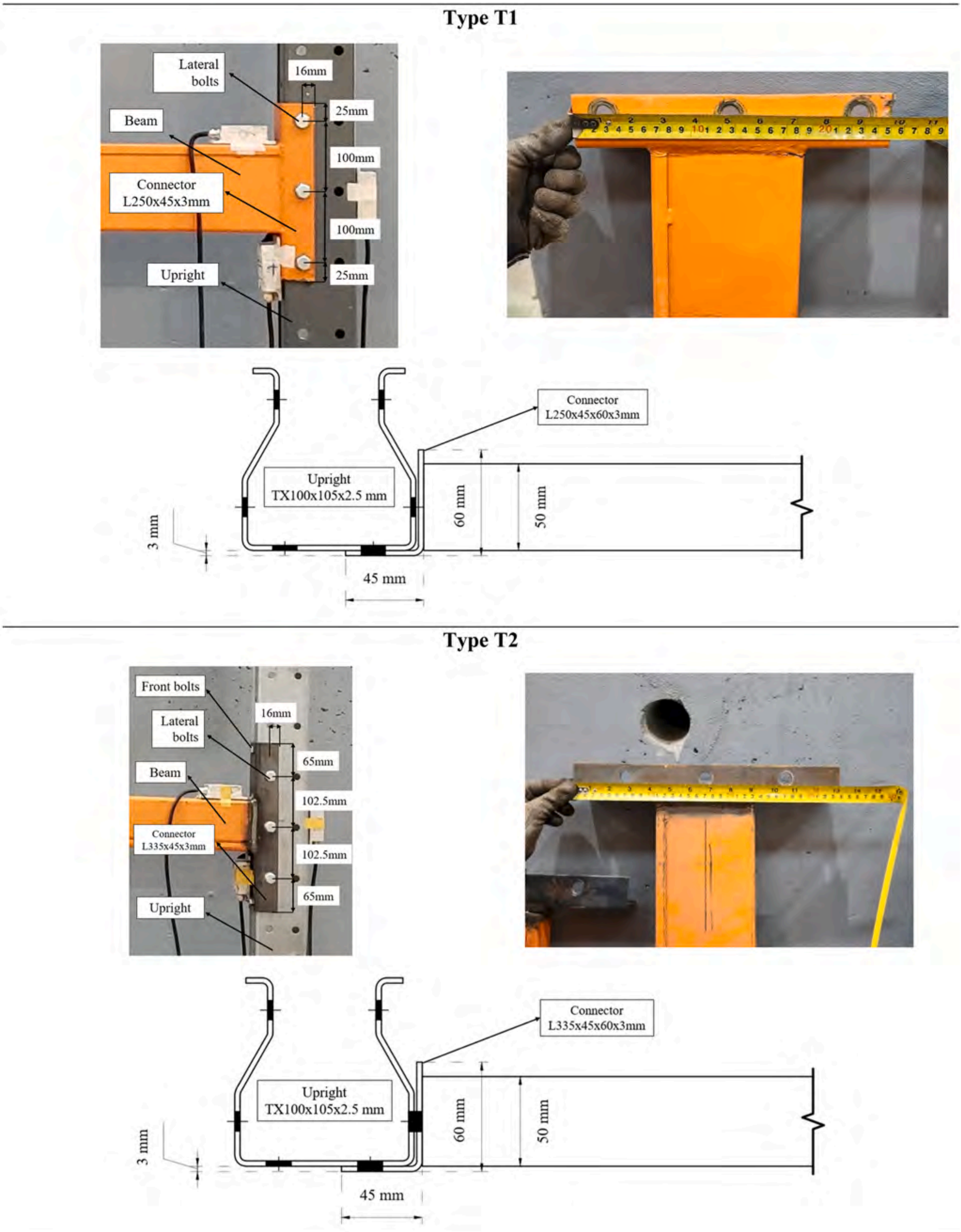

Fig. 1. Two types of beam-to-upright connections, T1 and T2.

Table 1
Summary of specimens tested.

Group	Test	Beam (mm)	Upright (mm)	L connector (mm)	Lateral Bolt (mm)	Front Bolt (mm)	Bolt Pretension
G1	#1	125×50×2	TX100×105×2.5	L45×250×3	3Φ12		Snug-tight
	#2	125×50×2	TX100×105×2.5	L45×250×3	3Φ12		Snug-tight
	#5	125×50×2	TX100×105×2.5	L45×250×3	3Φ12		Snug-tight
	#3	125×50×2	TX100×105×2.5	L45×250×3	3Φ12		70 %
	#4	125×50×2	TX100×105×2.5	L45×250×3	3Φ12		70 %
	#6	125×50×2	TX100×105×2.5	L45×250×3	3Φ12		70 %
G2	#7	125×50×2	TX100×105×2.5	L45×335×3	3Φ12	2Φ12	Snug-tight
	#8	125×50×2	TX100×105×2.5	L45×335×3	3Φ12	2Φ12	Snug-tight
	#9	125×50×2	TX100×105×2.5	L45×335×3	3Φ12	2Φ12	70 %
	#10	125×50×2	TX100×105×2.5	L45×335×3	3Φ12	2Φ12	70 %
G3	#11	100×50×2	TX100×105×2.5	L45×250×3	3Φ12		Snug-tight
	#12	100×50×2	TX100×105×2.5	L45×250×3	3Φ12		Snug-tight
	#13	100×50×2	TX100×105×2.5	L45×250×3	3Φ12		70 %
	#14	100×50×2	TX100×105×2.5	L45×250×3	3Φ12		70 %
G4	#15	100×50×2	TX100×105×2.5	L45×335×3	3Φ12	2Φ12	Snug-tight
	#16	100×50×2	TX100×105×2.5	L45×335×3	3Φ12	2Φ12	70 %

Research conducted by Sangle et al. [6] studied the elastic stability analysis of cold-formed pallet rack structures with semi-rigid connections. Experimental and numerical study have shown that stiffening of the open upright sections using the spacer bar, channel and hat as external stiffeners will considerably increase the load carrying capacity of the frames. Moreover, the Zhao et al. [7] investigates the flexural behavior of connections associated with the cold-formed steel storage pallet racks. The results showed that the deformation of the connections was dependent on the relative thickness between upright and the beam-end-connector.

Bernuzzi et al. [8,9] performed a comparative study on steel racks employing the European and United States approaches. In general, the European performance of isolated members always results less conservative than the US performance, with different values of the load capacity. The imperfection modelling technique has a negligible influence on the rack performance. Recently, the monotonic and cyclic response of speed-lock connections were studied by Yin et al. [10]. The bearing capacity and energy dissipation of several configurations under cyclic loading were studied experimentally using a cantilever test method. The results showed that additional bolts and welds significantly enhanced the capacities and deformability of the connections.

Posteriorly, an extensive review of the research performed in the last decades in the down-aisle direction was performed by Shah et al. [11]. The connection performance measures evaluated are the strength (moment resistance), rigidity (rotational stiffness) and ductility (rotational capacity) of the beam end connector. Zhao et al. [12] presented a mechanical model based on the component method to predict the initial rotational stiffness of beam-to-upright connections in cold-formed steel storage racks. The proposed model can be only used to obtain the initial rotational stiffness of beam-to-Upright connections and the initial stiffness is an upper limit of a connection stiffness, and it cannot be used in design. Additionality, Gusella et al. [13] studied the beam-column joints of industrial pallet racks using monotonic and cyclic tests through experimental research. The experimental results confirmed that the racks connections are significantly different from traditional steel framed buildings due to pinching in hysteresis loops.

Moreover, the cyclic performance of steel storage rack beam-to-upright bolted connections were studied by Dai et al. [14,15]. The results showed that three failure modes were observed in the tests: connector crack, local buckling of the upright and beam-end-failure. However combined failure can be obtained. The influence of mechanical and geometric uncertainty on racks and the evaluation of mechanical properties were studied by Gusella et al. [16,17]. The results indicated that system effects reduce flexural stiffness and the variability in the response of individual components does not propagate to the overall flexural capacity.

As observed several research conducted experimental studies to characterize the hysteretic behavior of steel rack connections. A high variability in the results was obtained in the results for different size of beam, column, connector, and number of bolts according to the conducted by [18–29]. These parameters have a high influence in the structural response of racks subjected to seismic forces. However, the use of bolted connections, without hooks, considering the behavior of the connection with pretensioned bolts as a strategy for improving its cyclic behavior has not been studied. Although bolt pretension is not common in the rack industry, its easy application can improve the performance of the system under lateral loads.

This paper is aimed in the assessment of cyclic performance of beam-to-upright connection considering the bolt pretension. In this sense, typical joint configurations with beam connected to Upright are studied considering the bolt pretension in comparison to those without pretension in the bolts. To achieve this goal, an extensive experimental study of steel storage racks connections with different sizes considering pretension and no pretension of bolts subjected to cyclic load was performed.

2. Experimental program

2.1. Connection types, dimensions, and material properties

In this investigation, two joint configurations of steel beam-to-upright bolted connections are evaluated. Two different beam sizes (TC100×50×2mm and TC125×50×2mm) and one column (TX100×105×2.5 mm) were used in the tests. The sections are typically used in the designs according to the practice in Chile. The tested configuration corresponds to the connection of a beam with a column, as shown in Fig. 1.

To evaluate the cyclic behavior of beam-to-upright bolted connections two different type of joint configurations were studied. The joint type T1 is a configuration with beam connected to upright through steel connector with L shape welded to beam and bolted to upright using three lateral bolts, while the joint type T2 is a similar configuration with two front bolts added to L-connector.

To study the influence of bolt pretension on the cyclic response, joints with bolts pretensioned and no pretensioned (snug-tight) were tested. Table 1 shows a summary of specimens tested. The weld used in the specimens was welded all around the beam with fillet welds and $D_w = 4$ mm.

Cold-formed steel members (beam, upright, L connector) were fabricated from ASTM A36 [30], while ASTM A325 [31] was used for bolts. The L connector was joined to beam using fillet welding all-around of beam. A bolt pretension of 70 % (49 kN) according to established in [32] was used. The material properties were obtained from coupon

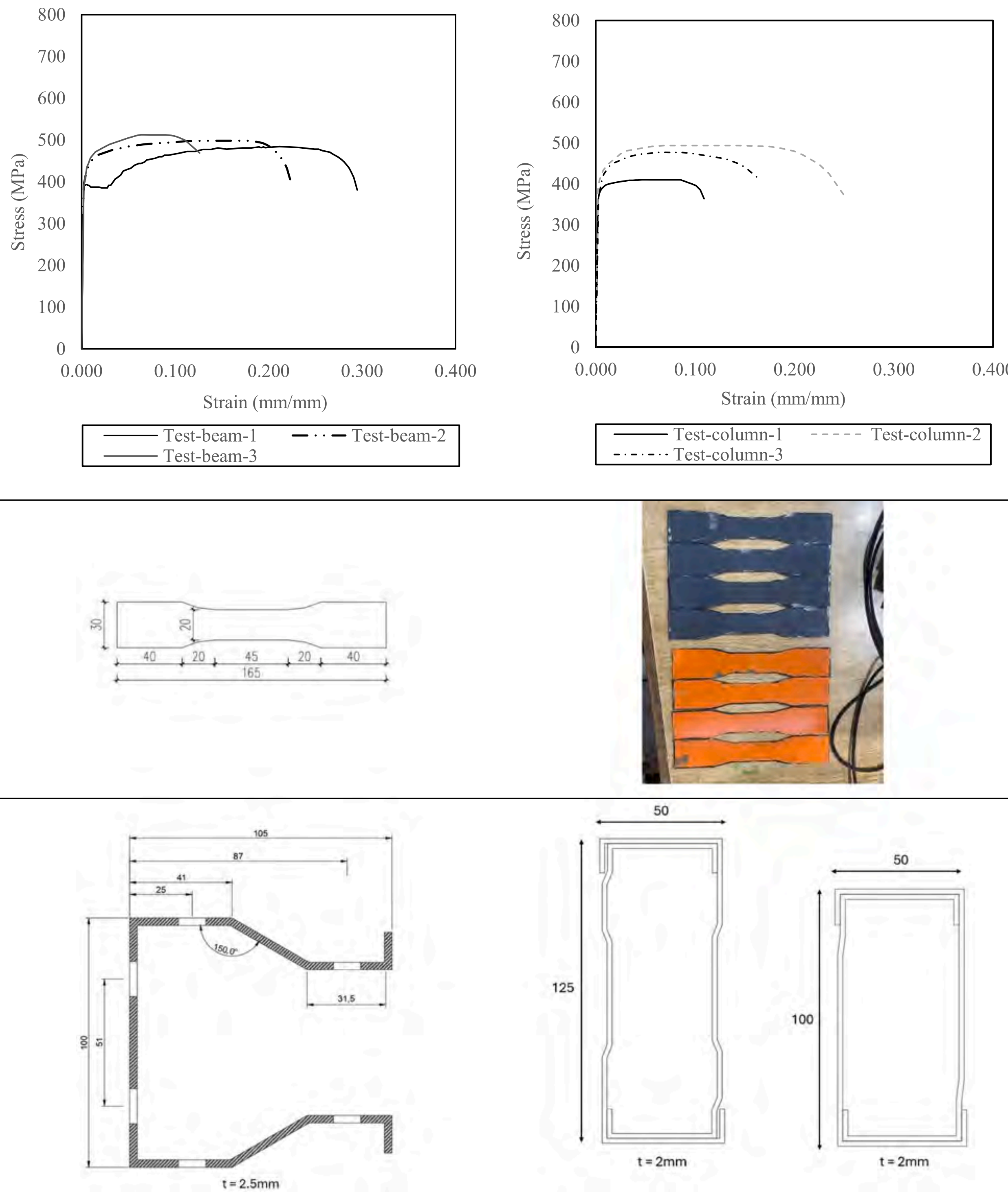

TX100x105x2.5 A=833 mm^2; Ix=1184x10^3 mm^4; Iy=1121.5 x10^3 mm^4; Sx=23.79x10^3 mm^3; Sy=17.64 x10^3 mm^3; rx=37.6 mm; ry=36.7 mm

TC125x50x2.5 A=946 mm^2; Ix=2195x10^3 mm^4; Iy=361x10^3 mm^4; Sx=35x10^3 mm^3; Sy=14x10^3 mm^3; rx=48 mm; ry=19.5 mm

TC100x50x2.5 A=847 mm^2; Ix=1302x10^3 mm^4; Iy=325x10^3 mm^4; Sx=26x10^3 mm^3; Sy=12 x10^3 mm^3; rx=39.2 mm; ry=19.6 mm

Fig. 2. Steel coupons specimen's dimensions, sections and material curves.

Table 2
Material properties for steel.

Element	Thickness (mm)	*fy* (*MPa*)	*Fu* (*MPa*)	$E_{average}$ (*MPa*)
Beam	2	392.5	484	
Beam	2	405	498	176692
Beam	2	407	512	
Upright	2.5	383	410	
Upright	2.5	421	493	177220
Upright	2.5	409	477	

tensile tests (see Fig. 2). A summary of the material properties is shown in the Table 2.

2.2. Test setup and instrumentation

The test setup was designed for full-scale testing of sixteen configurations of steel rack joints subjected to cyclic loading. The tested joint assembly includes two pinned restraints at the end of columns to simulate points with zero moments and the application of a cyclic load at the beam end. In addition, a lateral restraint was used to prevent out-of-plane displacement of the beam by the applied displacement. The load is applied by an actuator with capacity of 147 kN connected to the reaction wall. Load cell, inclinometers, and transducers (LVDT) were used. The load cell located at the point of load application to capture the applied force, the LVDT to measure the displacements applied at the beam end, and inclinometers to obtain the rotations at beam, upright and L-connector. In Fig. 3, experimental setup is shown.

2.3. Loading protocol

The cyclic loading is applied according to the loading protocol established in Seismic provisions [33]. This protocol consists of the application of cyclic displacements at the beam end, which are captured as force through the load cell. Fig. 3 shows the loading protocol used according to [33].

3. Experimental results

The results of the experimental study are shown and analyzed according to criteria of cyclic behavior, failure mechanism, dissipated energy and stiffness. Therefore, force vs. displacement (Δ) hysteresis curves, normalized moment vs. rotation (θ) curves, energy dissipated per cycle, normalized tangent stiffness vs. rotation (θ) and secant stiffness vs. rotation (θ) are reported. The normalized moment was calculated as M/M_y, where M is the acting moment and $M_y = F_y\, S_x$ (F_y, yield stress and S_x, is the section modulus). In addition, the energy dissipated per cycle, E, was calculated as the area under the curve of each cycle, while the secant stiffness, K_s, was calculated as the slope measured at each unloading of each loading cycle under positive and negative actions. Also, the stiffnesses was normalized by the initial stiffness K_o, calculated as the slope at the initial cycles. For a proper comparison, similar joint configurations will be grouped. This allows to evaluate the influence of the pretension on the bolts considering different beams, number, and location of bolts. A summary of key parameters is shown in Table 3.

In Fig. 4, the maximum moment normalized to the yield moment vs. the maximum rotation achieved by each connection is reported. Connections without pretension are shown in blue while connection with pretensioned bolts are shown in red. The configurations with pretensioned bolts reached average resistance values of $\overline{M_{\max}/M_y} = 0.79$, while joint configurations without pretension achieved average resistance values of $\overline{M_{\max}/M_y} = 0.73$. In terms of strength, higher average rotation values were also reported for connections with pretensioned bolts ($\overline{\theta} = 0.08 rad$ vs. $\overline{\theta} = 0.07 rad$). It is important to highlight that the minimum resistances and rotations were developed for the connections without pretensioned bolts, $(M_{\max}/M_y)_{\min} = 0.63$ y $\theta_{\min} = 0.05 rad$. These results confirm the clear effect of bolt pretension in the cyclic performance of rack moment connections.

3.1. Hysteresis curve

The Fig. 5 shows the hysteresis curves and failure mechanism of specimens tested. In group G1, the maximum rotation and strength was achieved in specimens with pretensioned bolts. In this sense, a maximum rotation of 0.0825 rad was obtained in specimen #4 and #6. However, the initial stiffnesses remained between 111.37 kNm/rad and 169.91 kNm/rad. A similar behavior was obtained for groups G2, G3 and G4, which the specimens with pretensioned bolts achieved higher strengths and rotations.

Hysteretic pinching was developed in the specimens without front bolts (#1-#2-#3-#4-#5-#6-#11-#12-#13-#14). Therefore, steel rack connections with a combination of front and lateral bolts (#7-#8-#9-#10-#15-#16) showed better behavior limiting the buckling in the L-connector. On the other hand, comparing only connections with front and lateral bolts (G2 and G4), the joint configurations without bolt pretension reached a lower strength, however, a failure in the weld with degradation of resistance was obtained for joints with bolts pretensioned once the maximum bending strength is reached.

Only the specimens with prestressed bolts #6, #10, #14 and #16 reached values greater than $0.8\, M_y$, therefore, the bolt pretension allows to improve the resistance of the steel rack connections subjected to cyclic loads. However, this performance is insufficient compared with the requirements established for buildings subjected to seismic loads.

3.2. Failure mechanism

Different failure mechanisms can be developed on steel rack connections, such as local buckling in the L-connector, local buckling in beam or upright, welding failure, bearing of bolts or shear failure in bolts. Mainly a single failure mechanism controlled by welding rupture in beams was achieved in specimens #2, #3, #5, #7, #8, #12, #14, #15 and #16. This explains the limited hysteretic behavior developed by the connections from the variability of welding process. Furthermore, a combined failure mechanism controlled by local buckling and rupture of welding was reached by the specimens #1, #4, #9, #10, #11 and #13. Finally, the specimen #6 exhibited a combined failure mechanism characterized by local buckling of L-connector and beam web, and posterior to these limit states, the weld fracture. The response can be improved using more robust sections with a distribution of bolts and connection elements with better strength, however, such actions are contrary to the practice in the design of this type of structures where the use of slender sections, structural configurations with high load levels and weak connections are commonly used.

3.3. Energy dissipation

The energy dissipation of the moment connection was obtained from the load-displacement curve and determined by calculating the area enclosed by each cycle as follow:

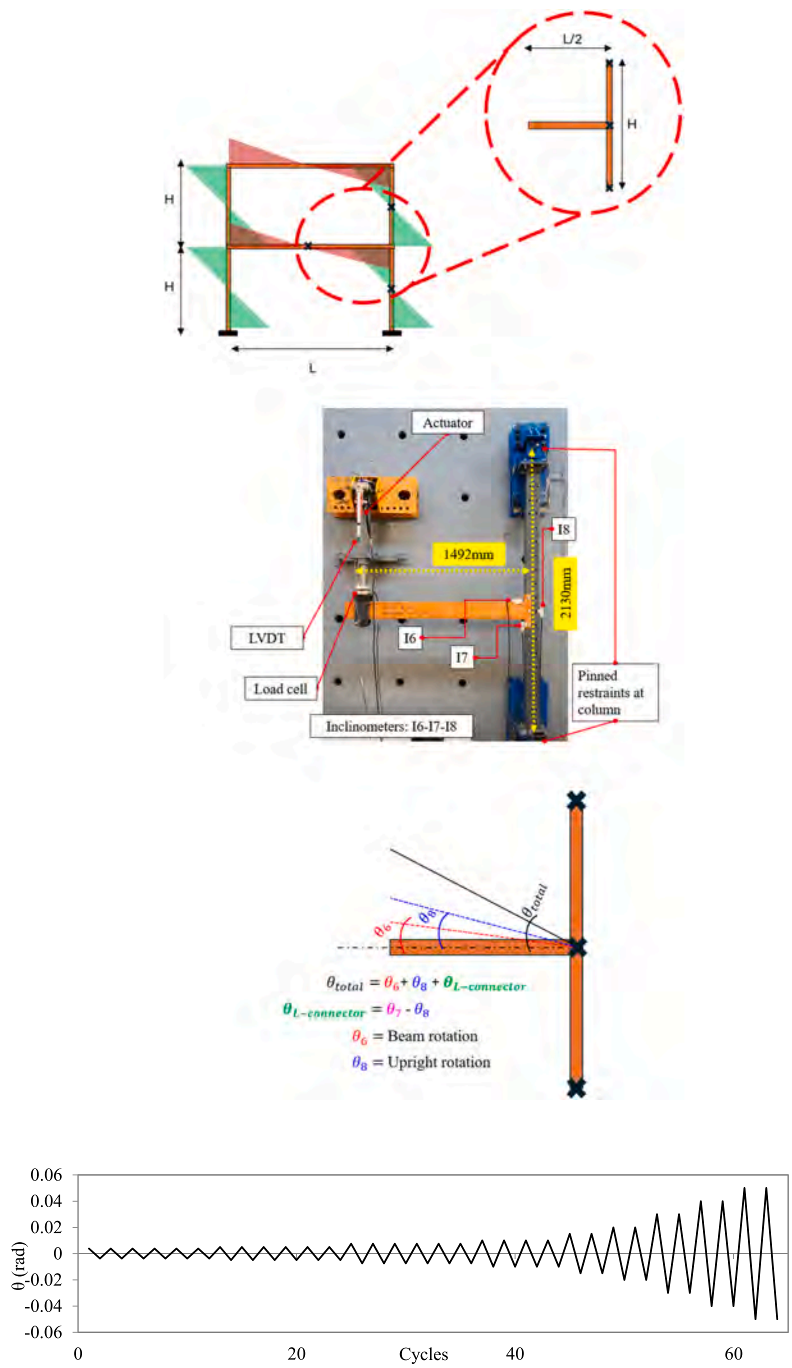

Note:

i) θ (rad): Interstory drift ratio in radians

ii) 0.00375 (6 cycles), 0.005 (6 cycles), 0.0075 (6 cycles), 0.01 (4 cycles), 0.015 (2 cycles), 0.02 (2 cycles), 0.03 (2 cycles), 0.04 (2 cycles), 0.05 (2 cycles), 0.06 (2 cycles)

Fig. 3. Experimental setup and displacement cyclic control according to Seismic Provisions [33].

Table 3
Summary of key parameters.

Group	Test	Ko (kN.m/rad)	M_{max}/M_y	θ_{max} (rad)
G1	#1	111.37	0.75	0.05
	#2	169.91	0.65	0.07
	#5	158.01	0.77	0.0725
	#3	164.91	0.75	0.07
	#4	133.04	0.7	0.0825
	#6	129.33	0.82	0.0825
G2	#7	181.06	0.76	0.073
	#8	95.11	0.63	0.073
	#9	134.19	0.78	0.073
	#10	160.66	0.83	0.072
G3	#11	82.48	0.7	0.0825
	#12	94.12	0.78	0.08
	#13	132.64	0.77	0.0825
	#14	125.11	0.83	0.084
G4	#15	130.64	0.76	0.081
	#16	126.69	0.86	0.0825

Note: θ_{max} = Maximum Rotation

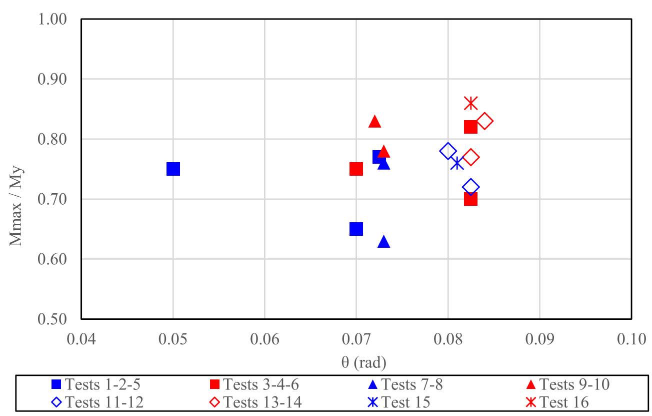

Fig. 4. Influence of bolt pretension in rack connections.

$$E_d = \int_{u_i}^{u_{i+1}} p(t)du \tag{1}$$

where u_i and u_{i+1} corresponding to displacements and $P_{(t)}$ is the force applied to the structure. Finally, the energy dissipation is presented as a cumulative energy dissipation. The dissipated energy is shown in Fig. 6.

3.3.1. Specimens of Group G1 (lateral bolts)

In the specimen #1, the energy dissipation is reached with similar slope up to 1 % drift; from this rotation level the buckling of beam web es started. Subsequently, dissipation is continued until fracture of the weld at 5 % drift. In the specimen #2, an upward pattern of energy dissipation was developed up to 6 % drift; also, the secant stiffness drops due to weld fracture without local buckling of beam. The specimen #5 achieved an incremental pattern of energy dissipation up to 7 % drift.

On the other hand, the specimen #3 reached an incremental pattern of energy dissipation up to 6 % drift, decreasing the slope of accumulated dissipated energy due to weld fracture. The specimen #4 achieved a similar pattern to specimen #3 up to 7 % drift. The specimen #6 exhibited a dissipation energy up to 8 % of rotation without changes of slope. The specimens with pretensioned bolts (#3-#4-#6) reached an average dissipated energy of 53 % higher in comparison to specimens without pretensioned bolts (#1-#2-#5).

3.3.2. Specimens of Group G2 (lateral and front bolts)

Specimens #7 and #8 show a symmetric pattern up to 6 % rotation, decreasing the energy dissipated up to 7 % drift due to fracture in the weld. The specimen #9 achieved a pattern similar to specimens #7 and #8, while the specimen #10 developed an incremental pattern of dissipation up to 8 % due to weld fracture. However, the specimens with pretensioned bolts (#9-#10) dissipated an average of 16 % higher in comparison to specimens without pretensioned bolts (#7-#8).

3.3.3. Specimens of Group G3 (lateral bolts)

Specimens #11-#12 and #13-#14 showed a similar incremental pattern of energy dissipation. The average of dissipated energy is 2.1 kJ for both sub-groups of moment connections; therefore, no influence of the bolt pretension can be concluded.

3.3.4. Specimens of Group G4 (lateral and front bolts)

Similar phenomenon was obtained for the specimens #15 and #16, which reached an average dissipation energy closer to 2.15 kJ. The energy dissipation levels do not show important differences; therefore, no influence of the bolt pretension effect can be concluded.

3.4. Stiffness

The measurement of secant stiffness is a tool to evaluate the cyclic performance in beam-to-upright rack connections. Fig. 7 shows the secant stiffness of the specimens tested. Specimens #1-#2-#5 (G1-bolts without pretension) developed a rapid stiffness drop, generally before 1 % drift. However, similar specimens #3-#4-#6 (G1-with pretensioned bolts), showed a more gradual and symmetrical stiffness drop. Therefore, the influence of bolt tightening on the cyclic response of the specimens in terms of secant stiffness can be observed. Also, specimens #7-#8 (G2-bolts without pretension) and #9-#10 (G2-with pretensioned bolts) exhibited an abrupt stiffness degradation pattern once the 0.00375 drift was exceeded.

Additionally, the stiffness degradation of specimens #11-#12 (G3-bolts without pretension) and #13-#14 (G3-with pretensioned bolts) show an asymmetric and abrupt trend once the 0.00375 drift is exceeded. Finally, specimens #15 and #16 without and with bolt pretension, respectively, showed a symmetric pattern of stiffness degradation and with a linear trend that had not been obtained in the rest of the specimens tested. It is important to highlight the high variability in the initial Ko stiffness obtained in the tests.

3.5. Cyclic rotation by component

The rotation in the components was captured from the installation of inclinometers that provide the rotation directly in the point of interest. As shown in Fig. 3, inclinometer I6 measures the rotation where the plastic hinge of the beam is expected. Inclinometer I7 was installed to

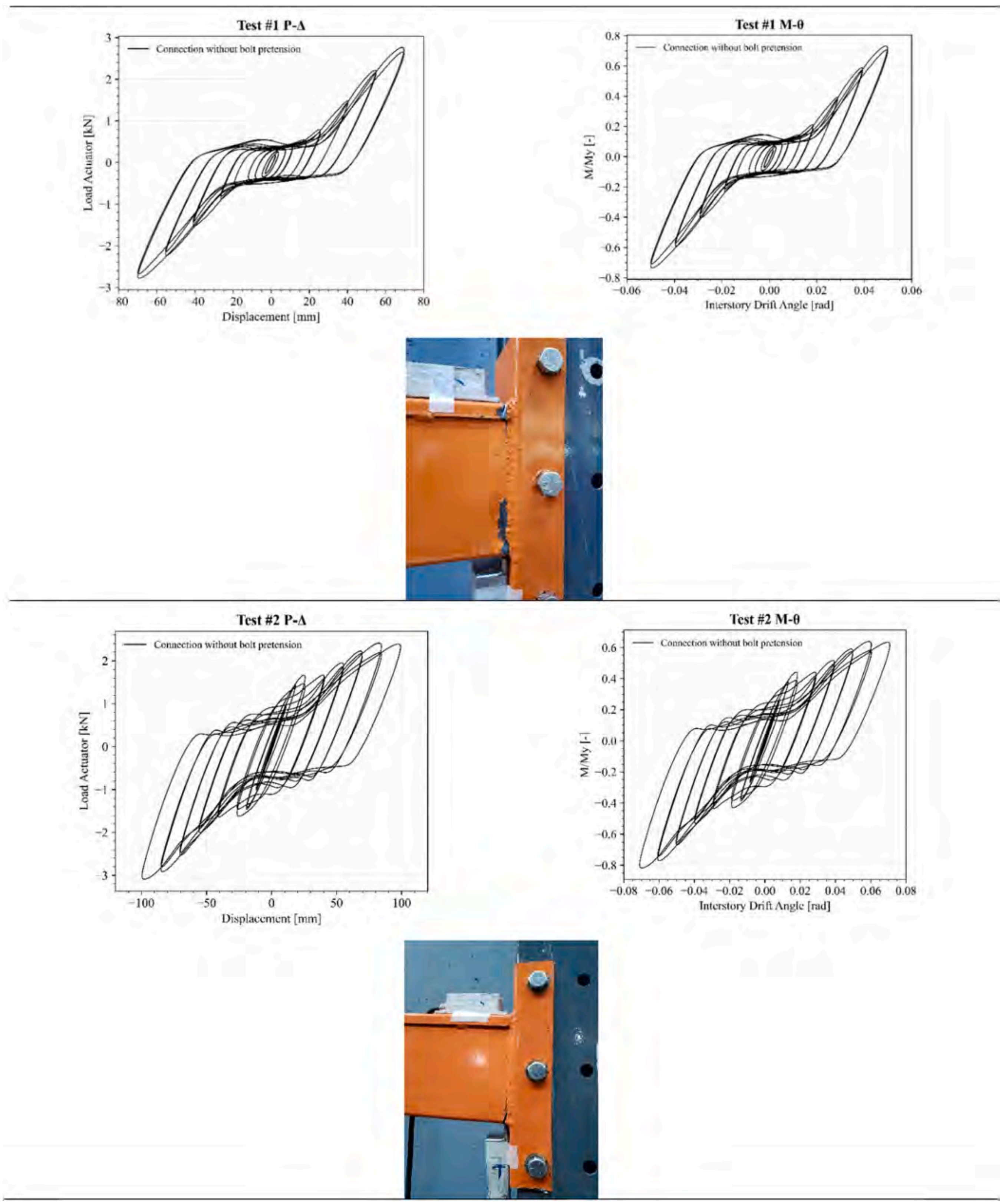

Fig. 5. Hysteresis curves and failure mechanism of specimens tested.

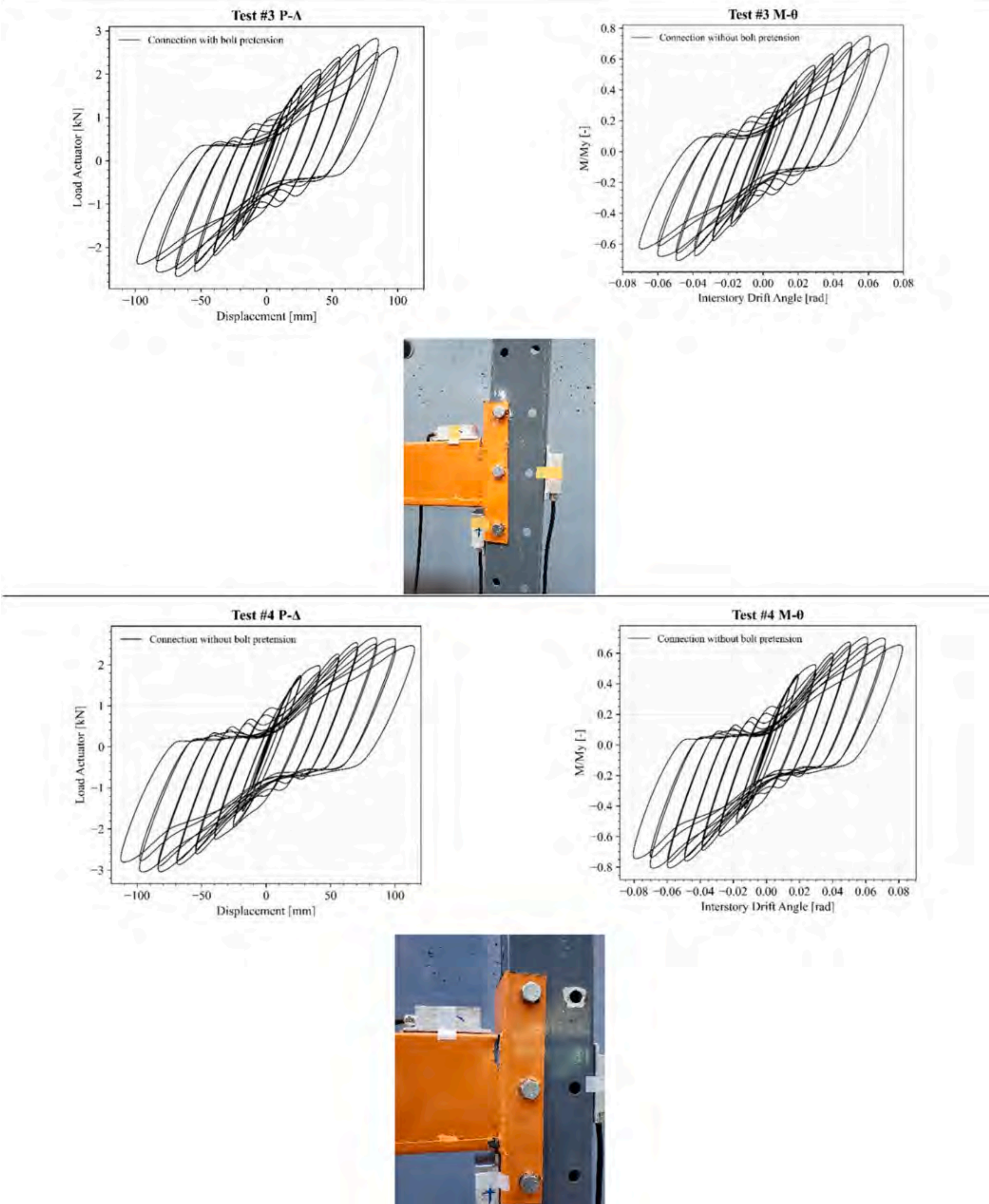

Fig. 5. (*continued*).

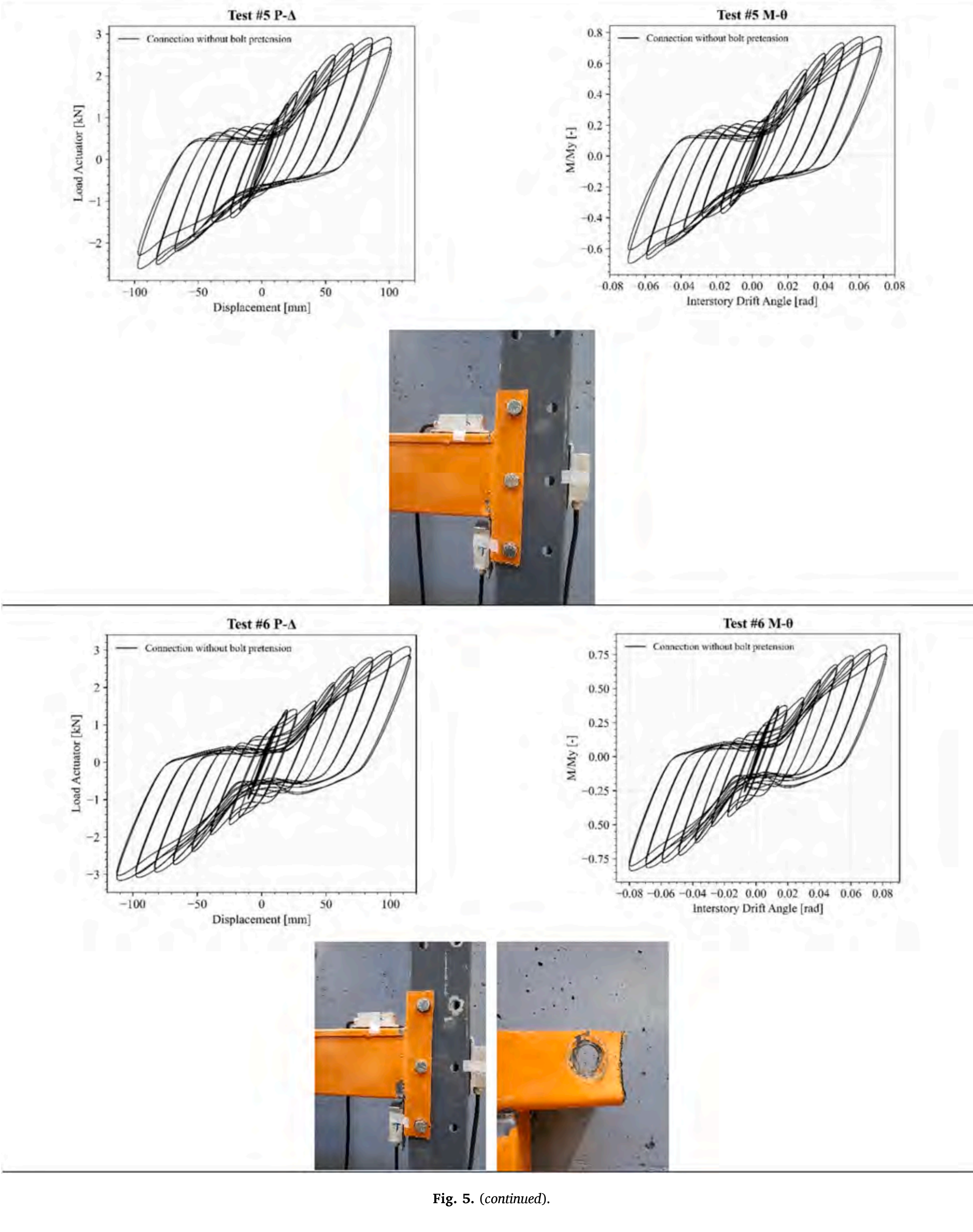

Fig. 5. (*continued*).

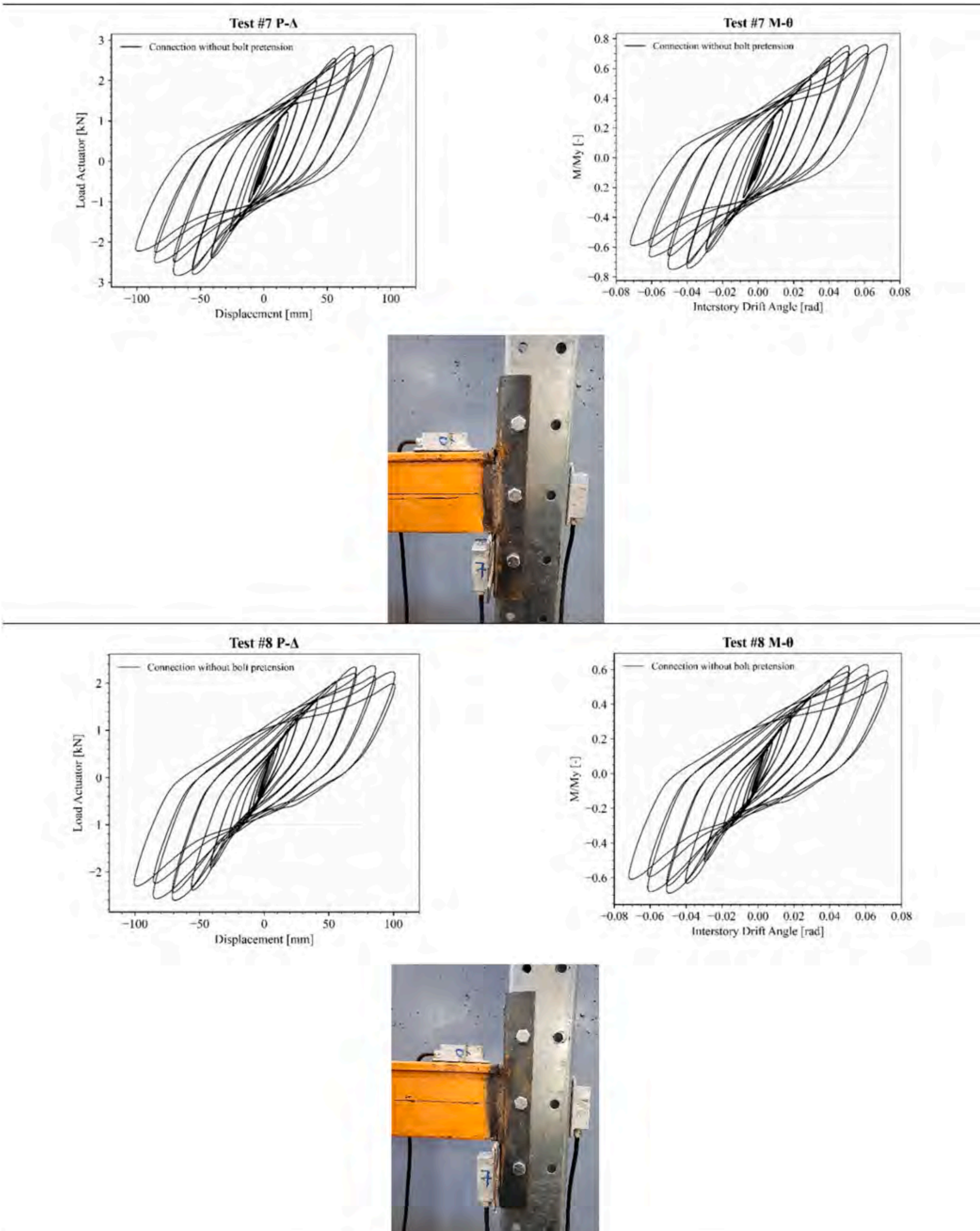

Fig. 5. (*continued*).

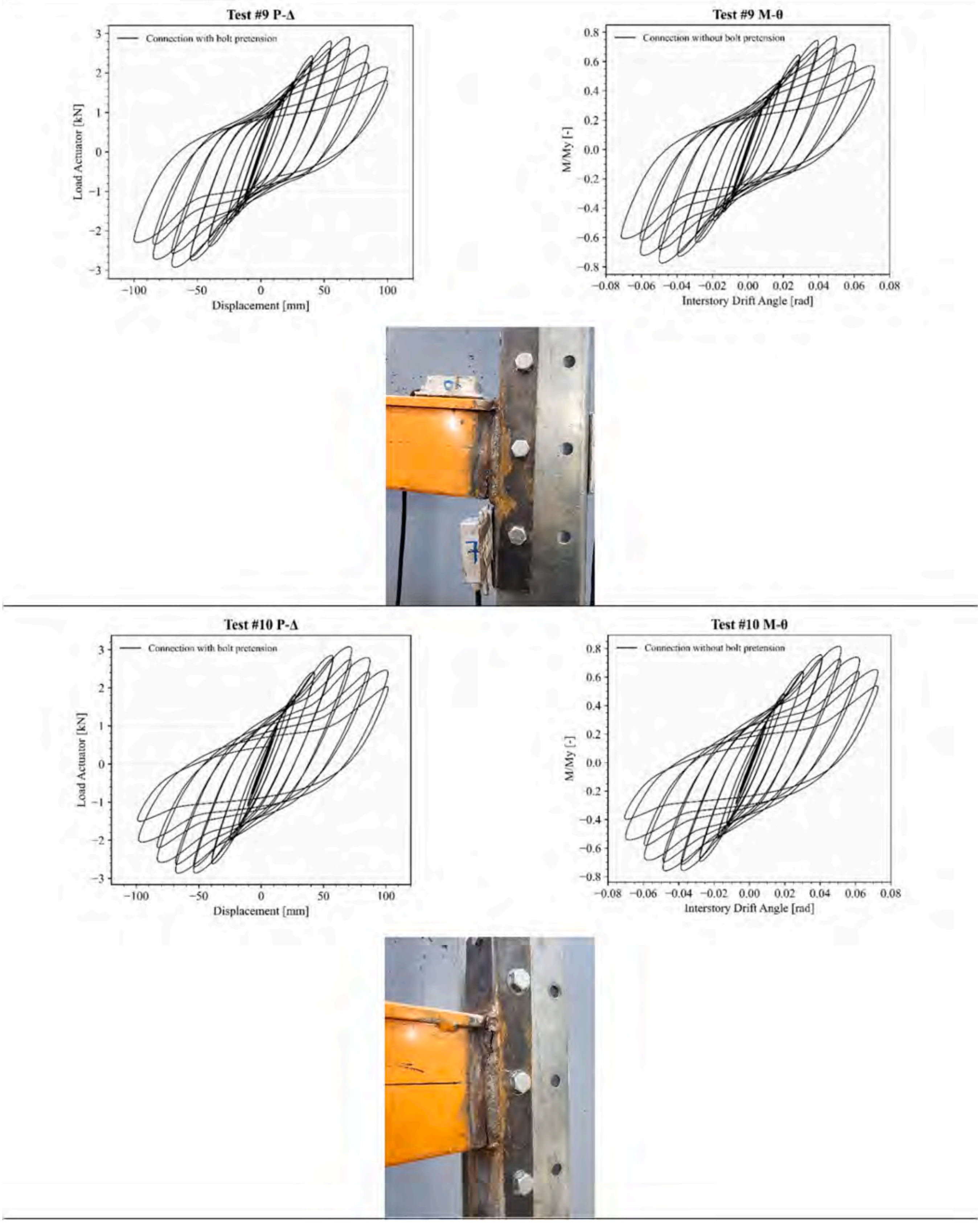

Fig. 5. (*continued*).

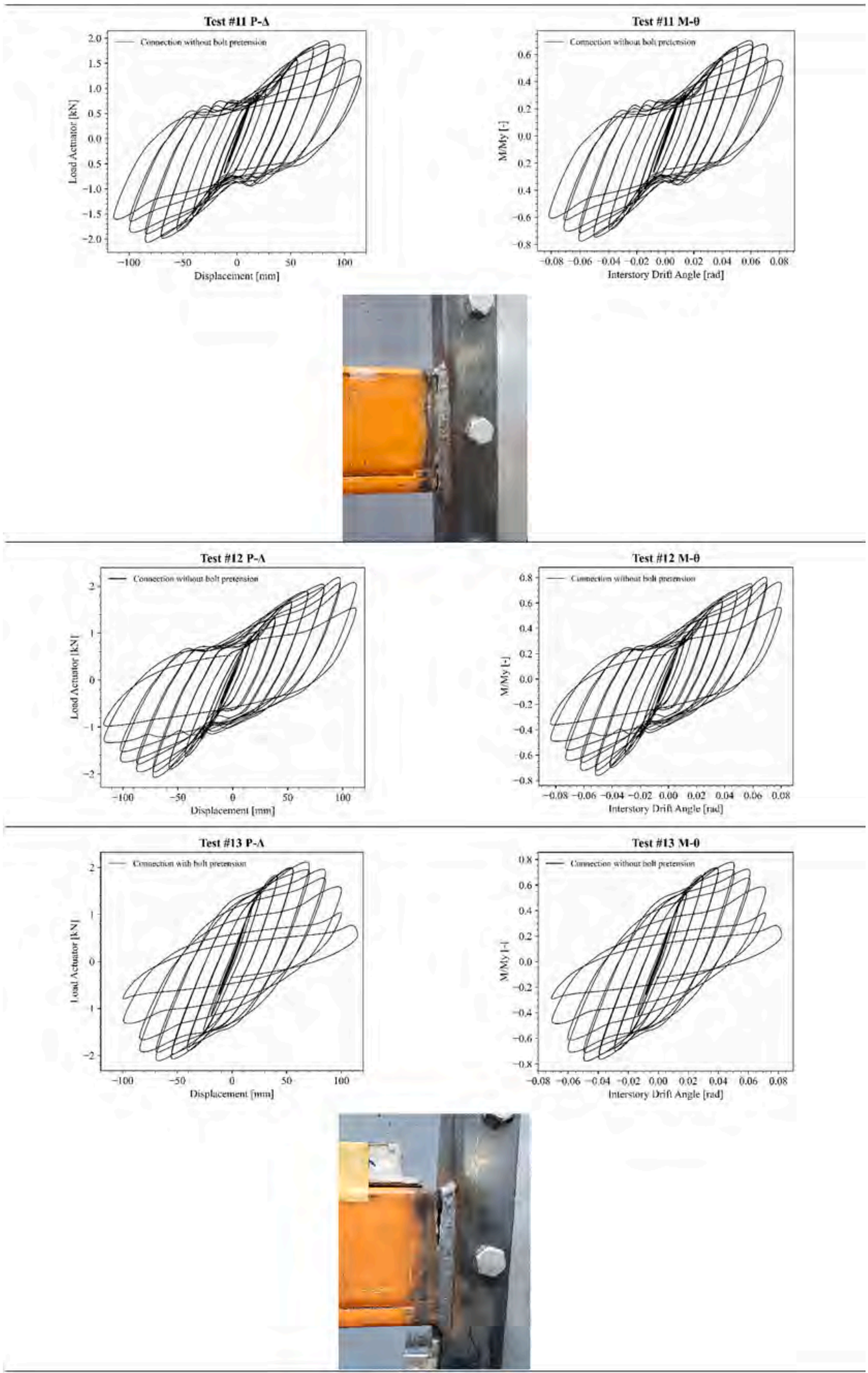

Fig. 5. (*continued*).

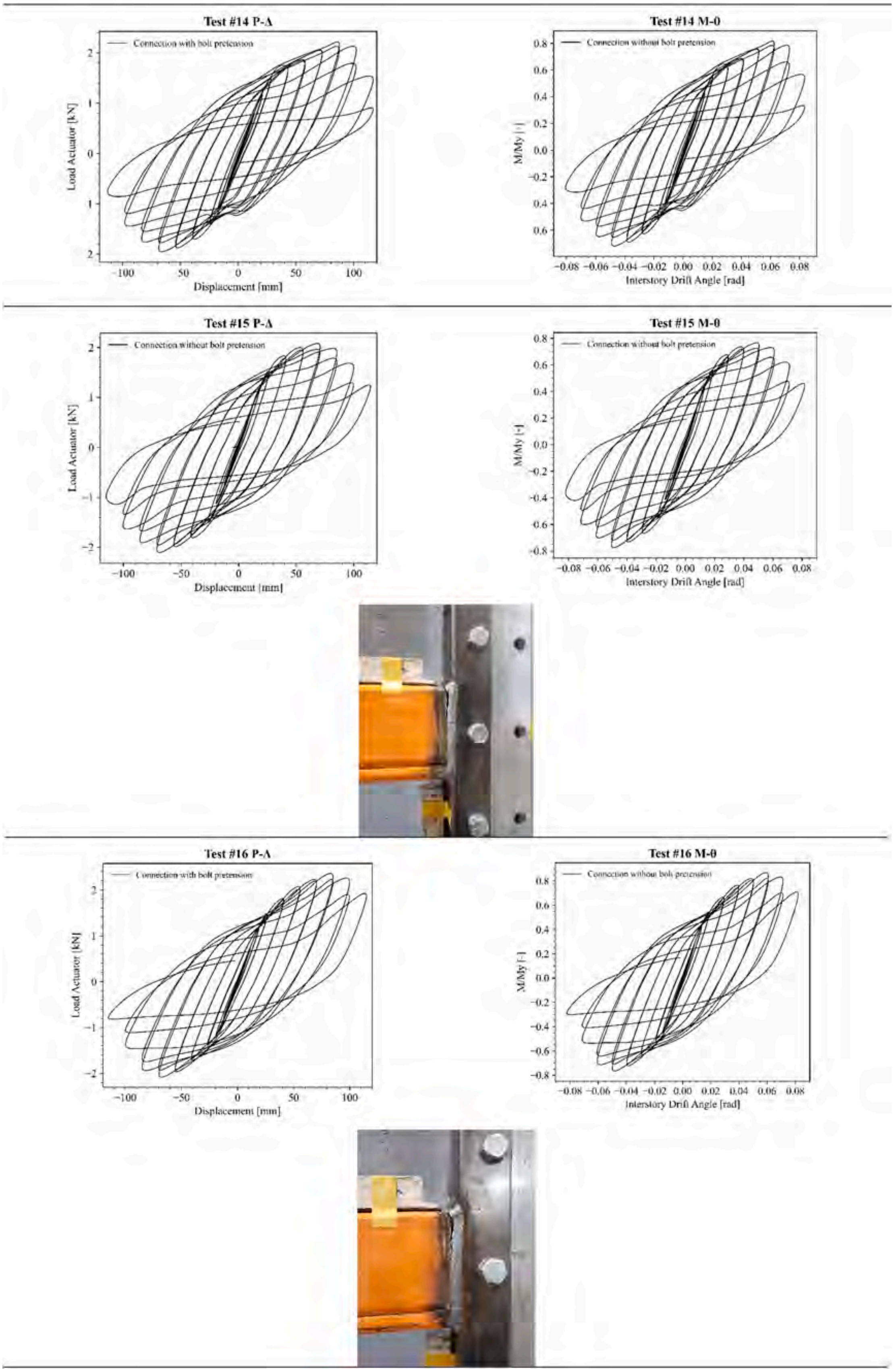

Fig. 5. (*continued*).

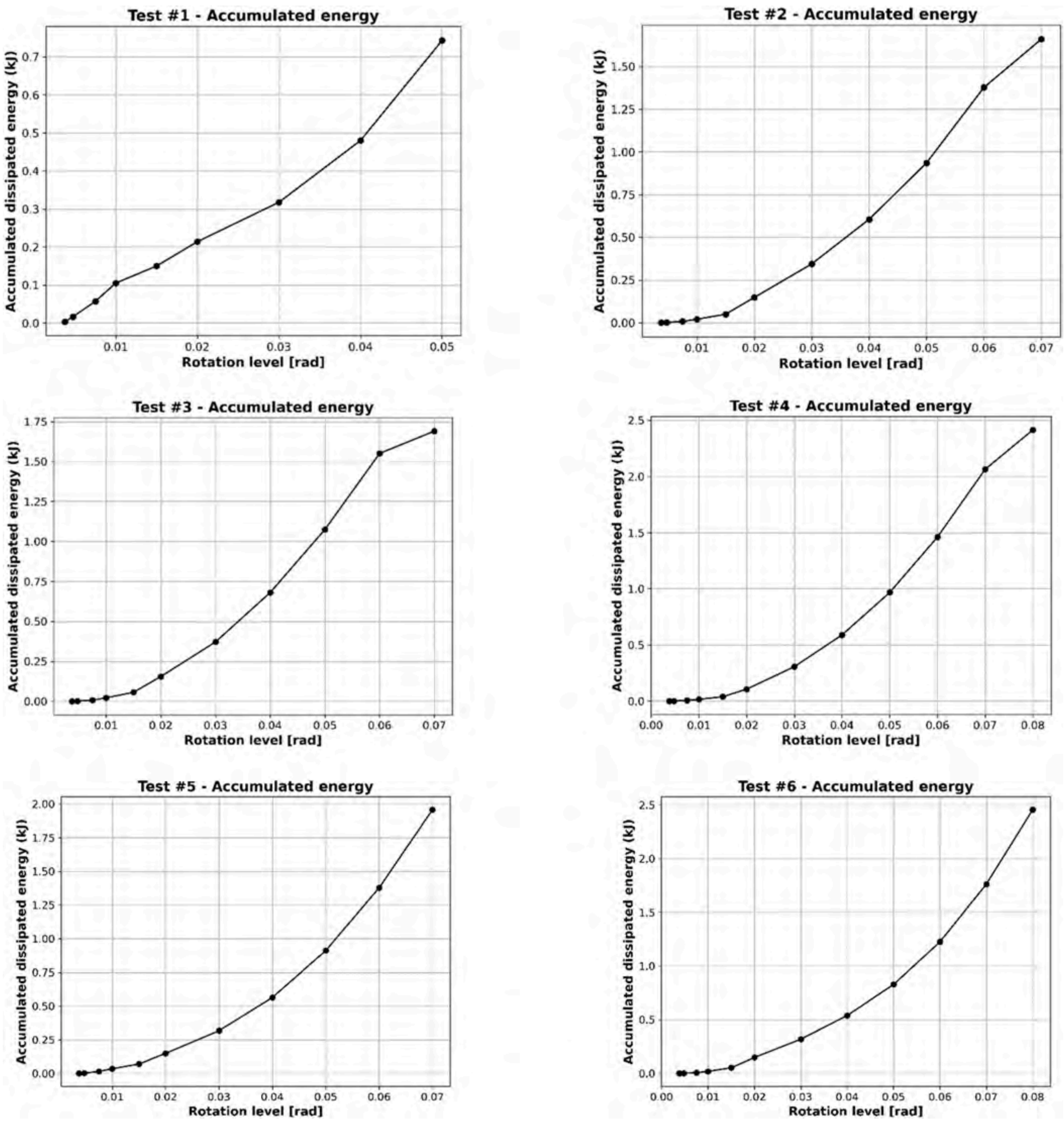

Fig. 6. Dissipated energy for joint configurations tested.

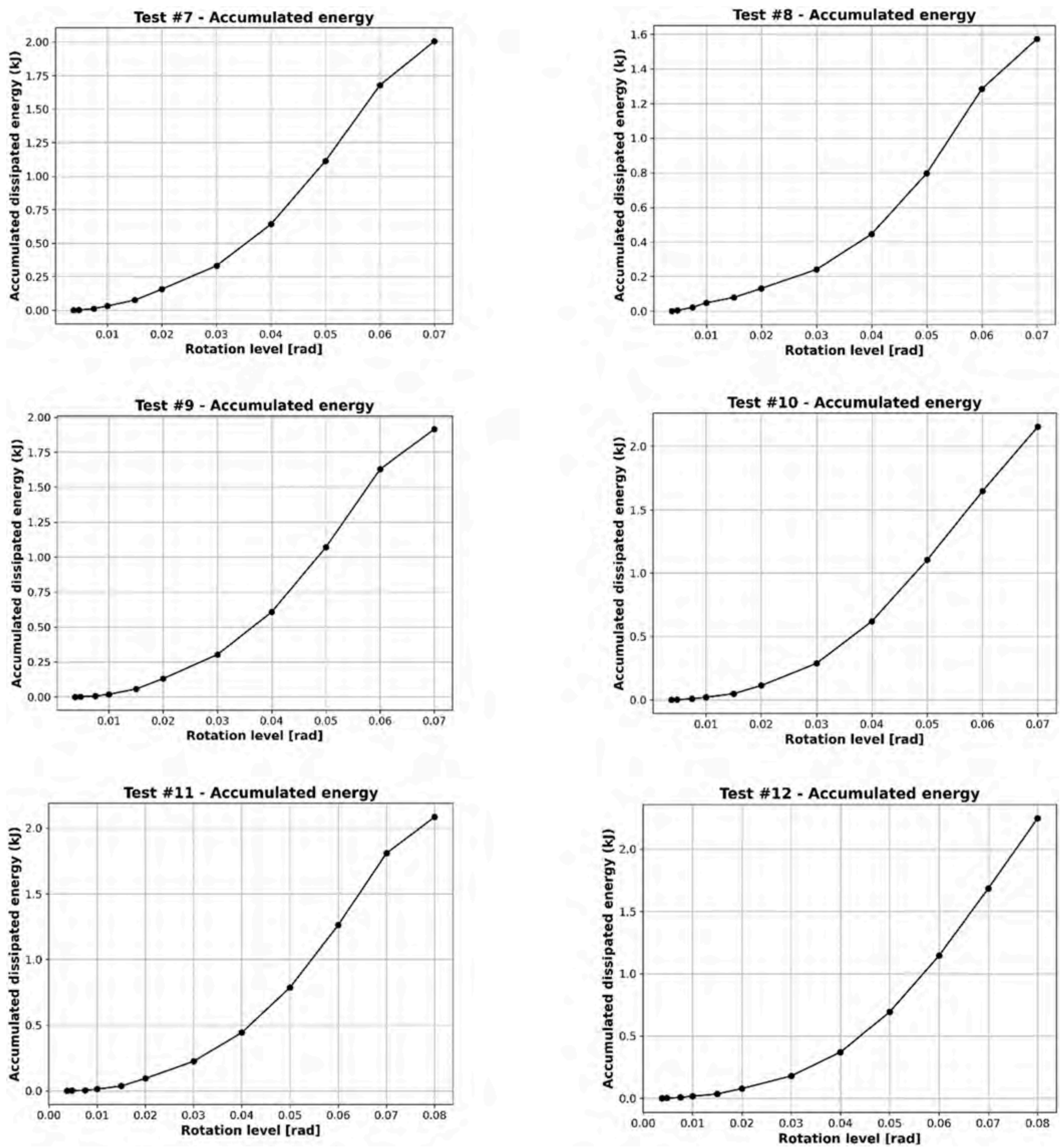

Fig. 6. (*continued*).

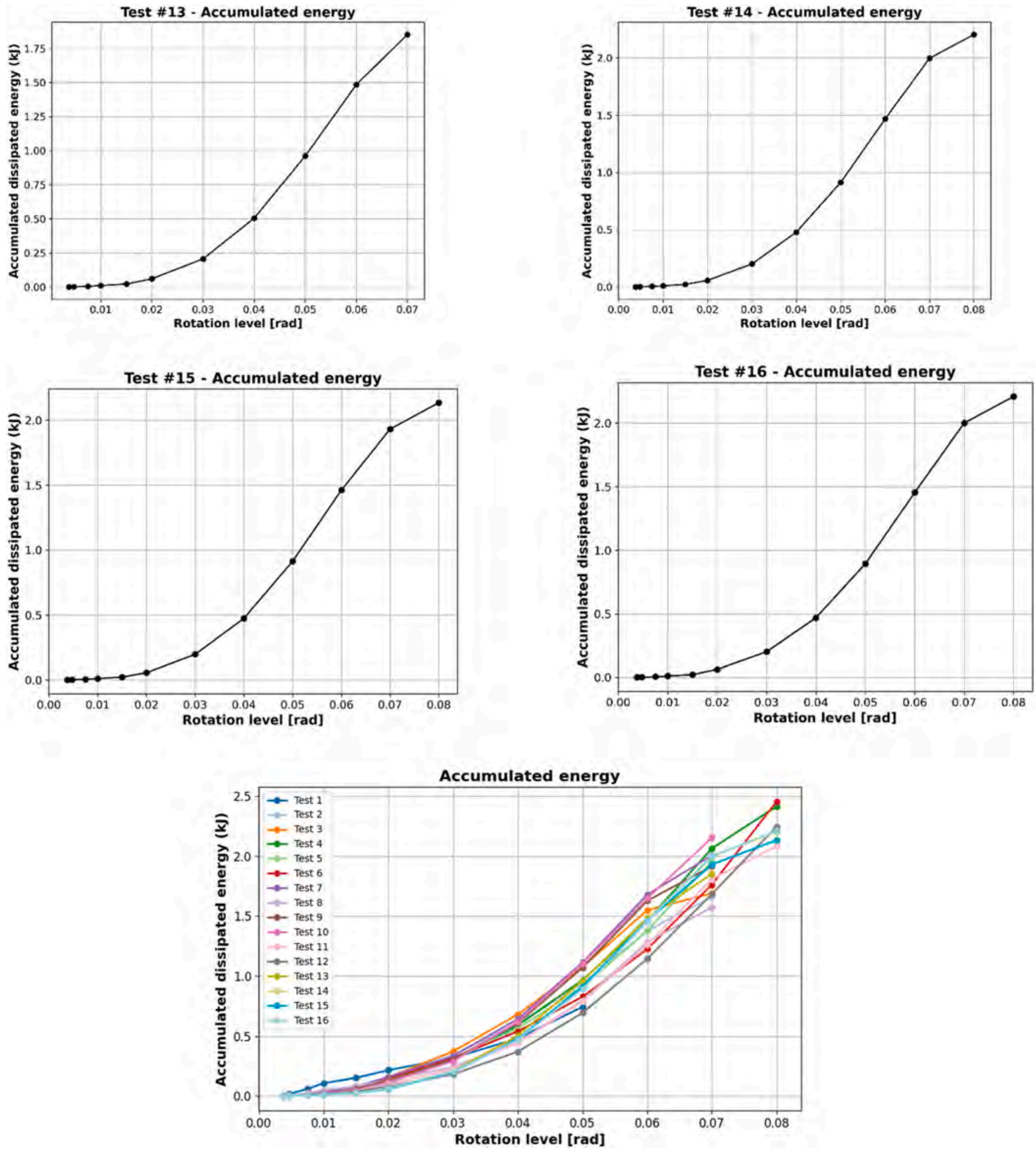

Fig. 6. (*continued*).

capture the rotation performed by the L-connector. While the inclinometer I8 was installed to measure the rotation developed by the column. As shown in Fig. 8, the rotations in the three inclinometers were measured for each specimen. In this sense, a low level of rotation was developed by the beam for all specimens tested. This corresponds with the damage pattern showed in the Fig. 5, where the typical failure was welding rupture and a limited local buckling in the beam for rotations above 5 %. This failure mechanism is not desired, however, no decoupling of components was reported, as can occur in hooked or speed lock rack connections [2,10,13].

The L-connector achieved higher rotation levels than the beam, however a significant influence of the front bolts was obtained. The shape of the curve in the specimens with lateral bolts showed a higher rotation at the L-connector with respect to the specimens with front bolts. This is due to the bracing generated by the front bolts to the L-connector, unlike the configuration with only side bolts where the deformation of the L-connector is not constrained. Additionally, a change in the slope of the curve occurs from cycles greater than 4 % in

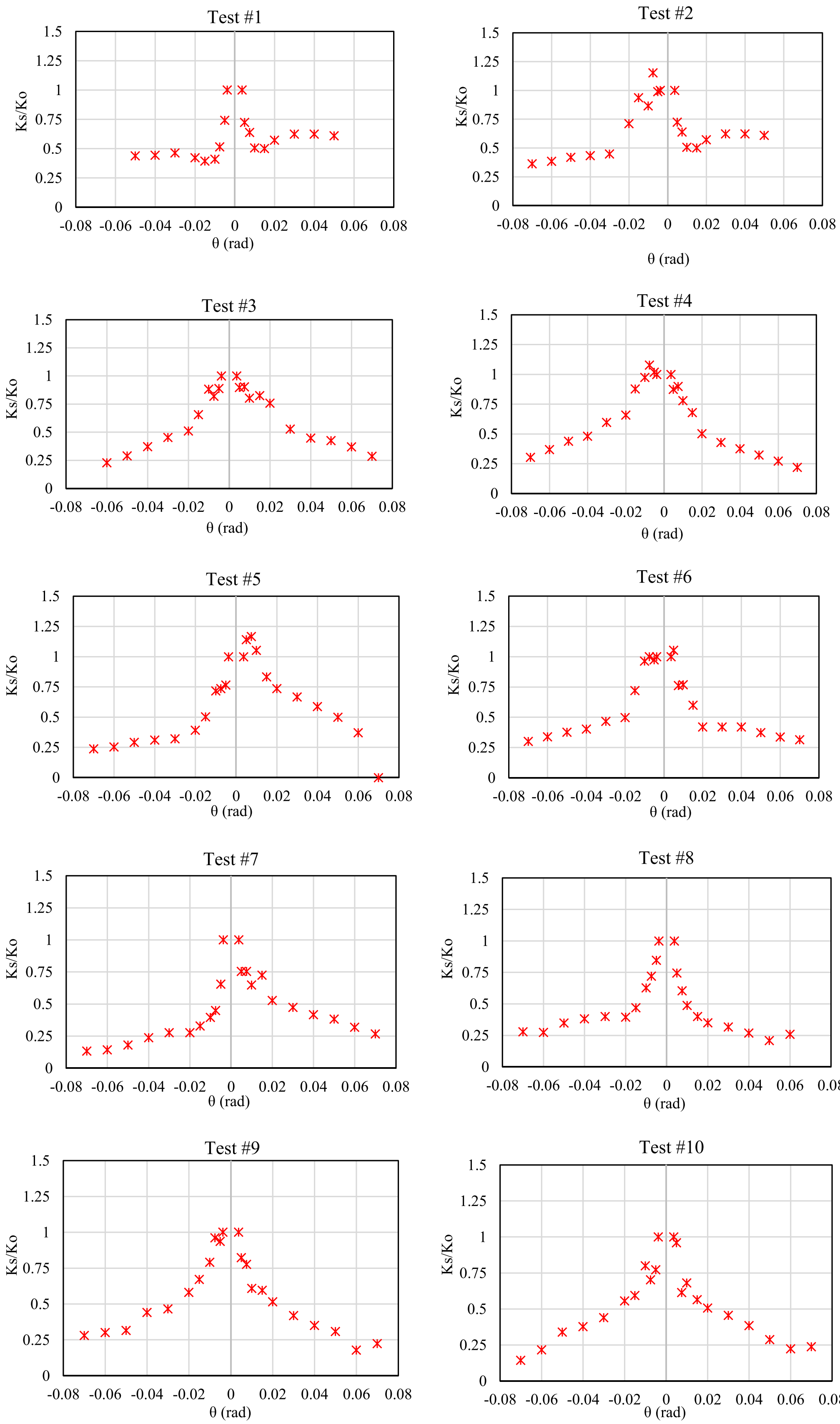

Fig. 7. Secant stiffness in specimens tested.

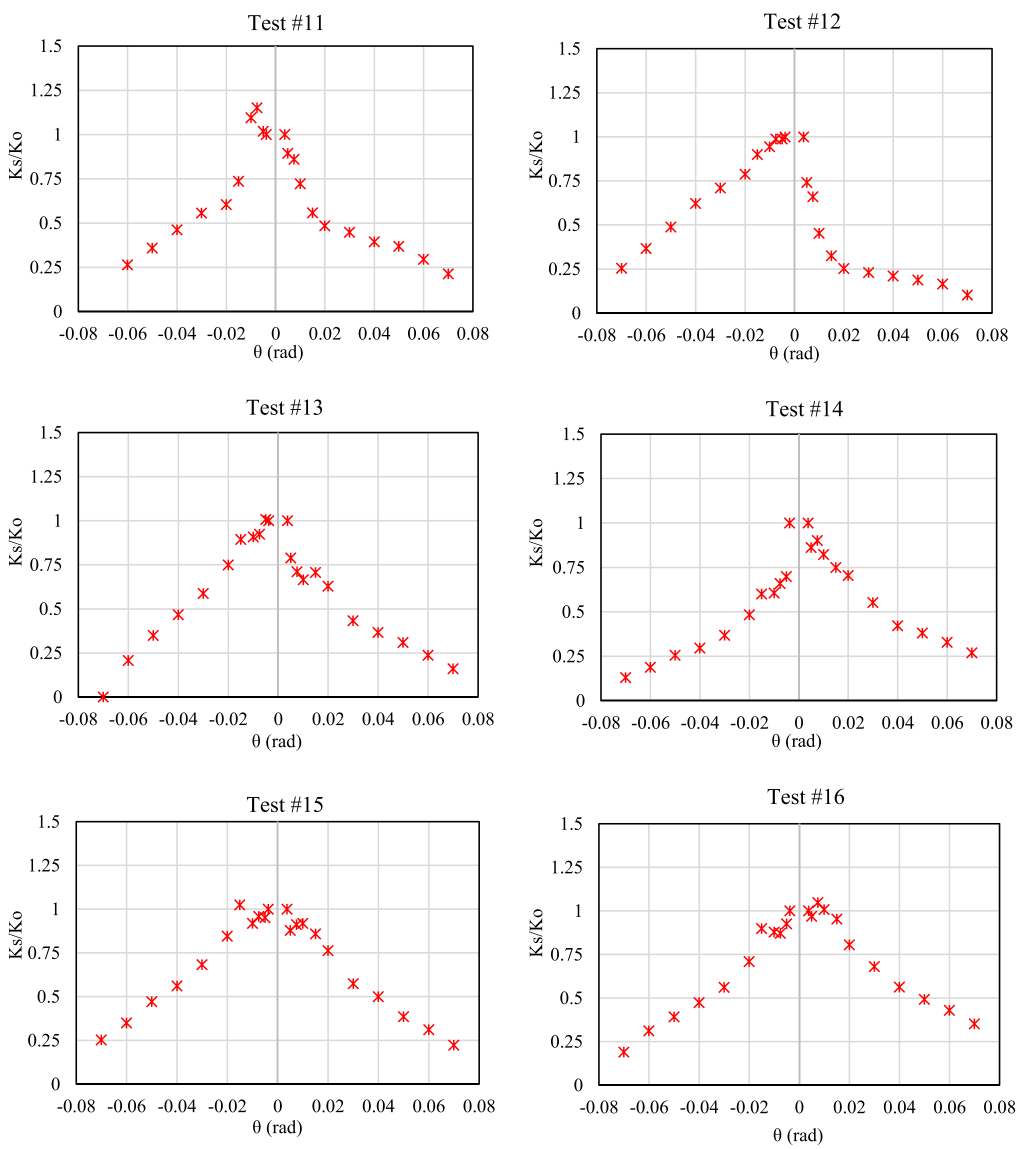

Fig. 7. (*continued*).

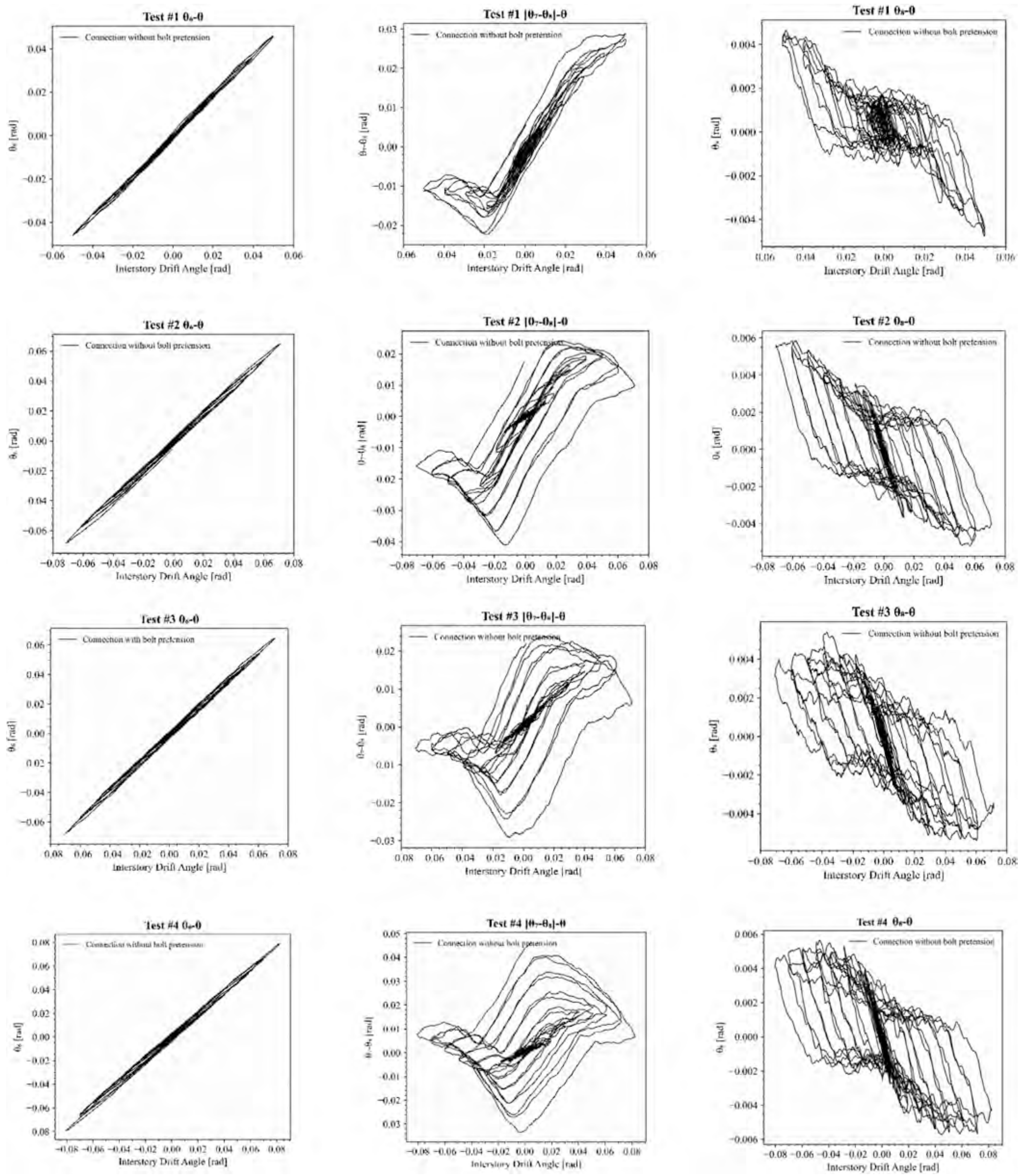

Fig. 8. Cyclic rotation of beam, L-connector and upright for specimens tested.

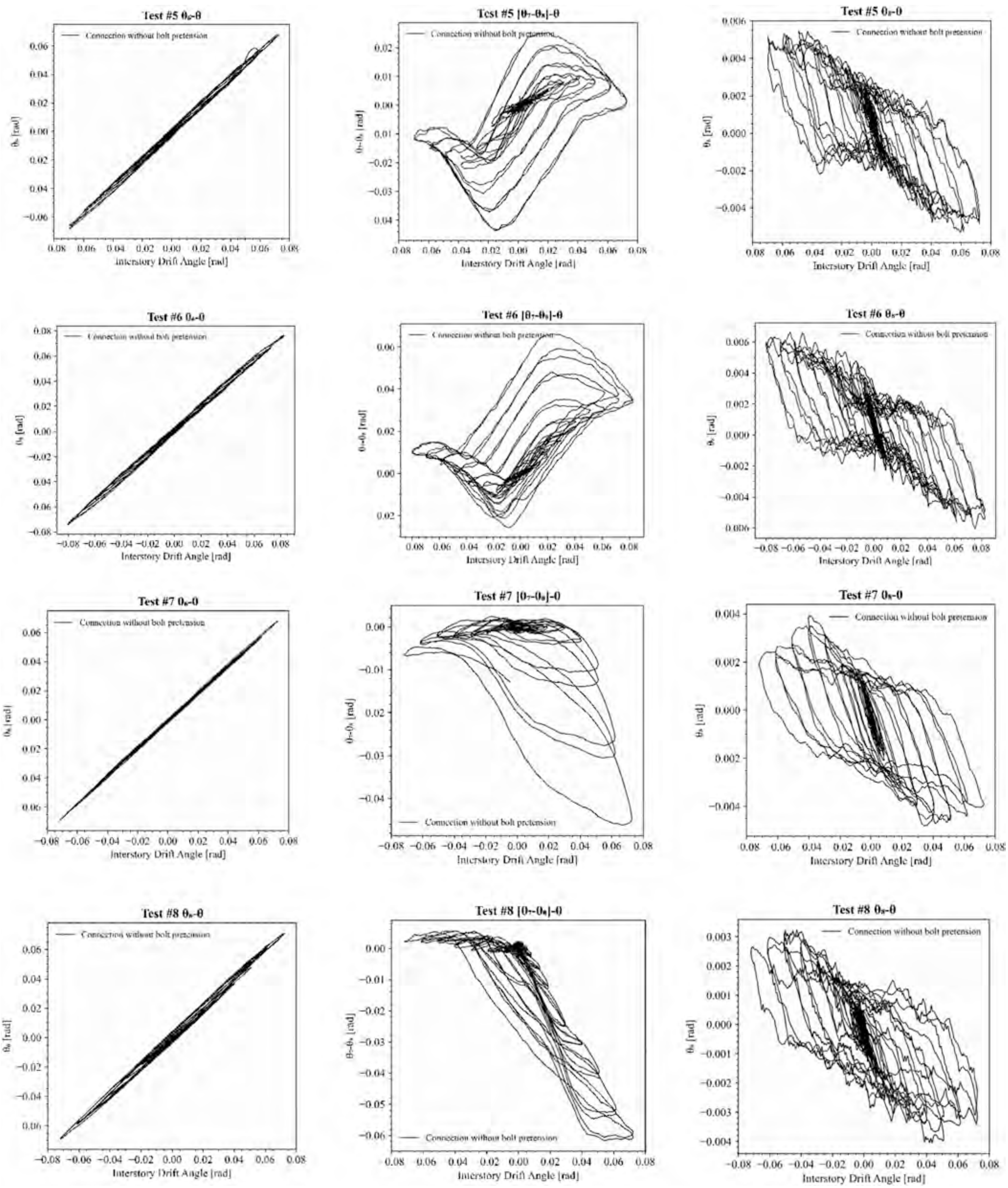

Fig. 8. (*continued*).

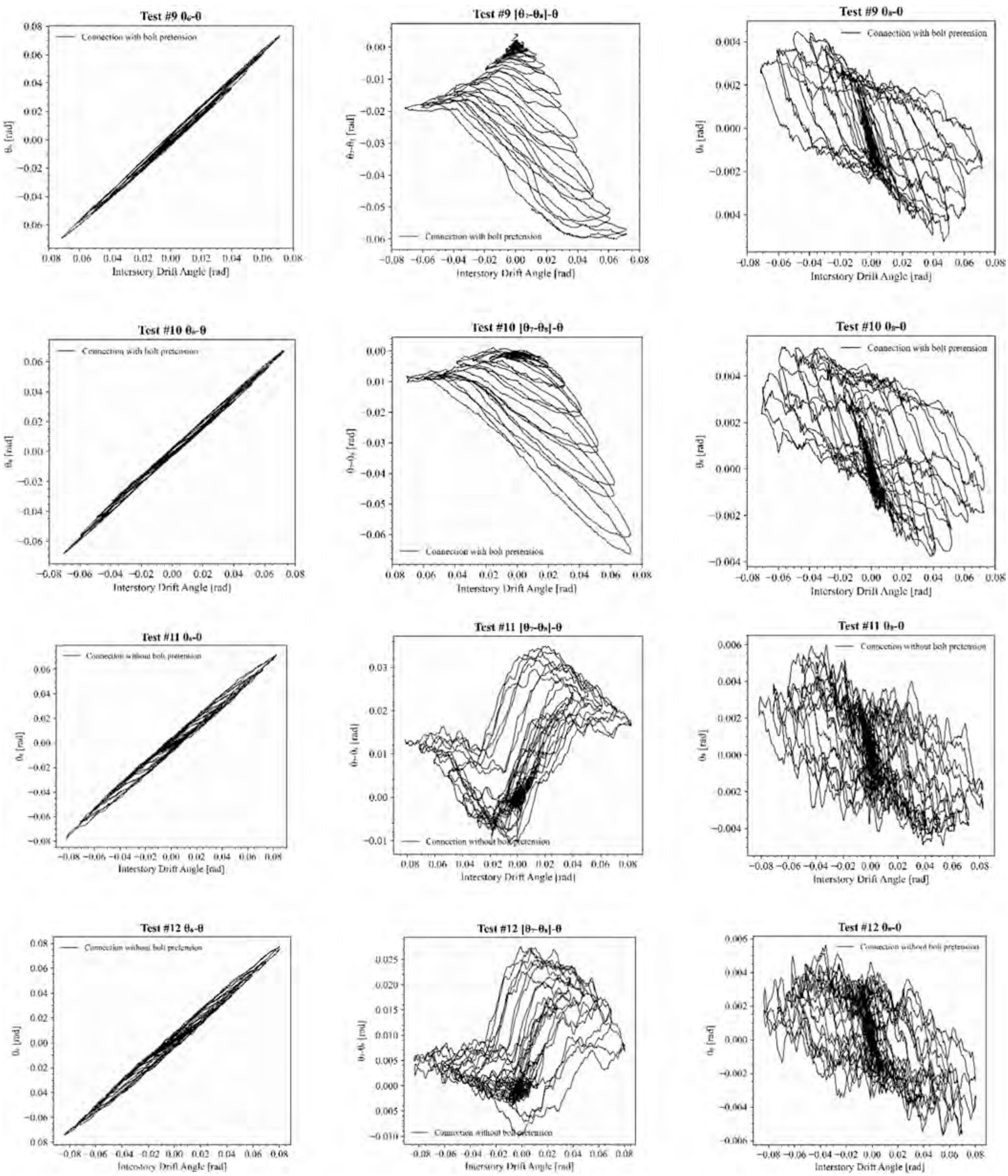

Fig. 8. (*continued*).

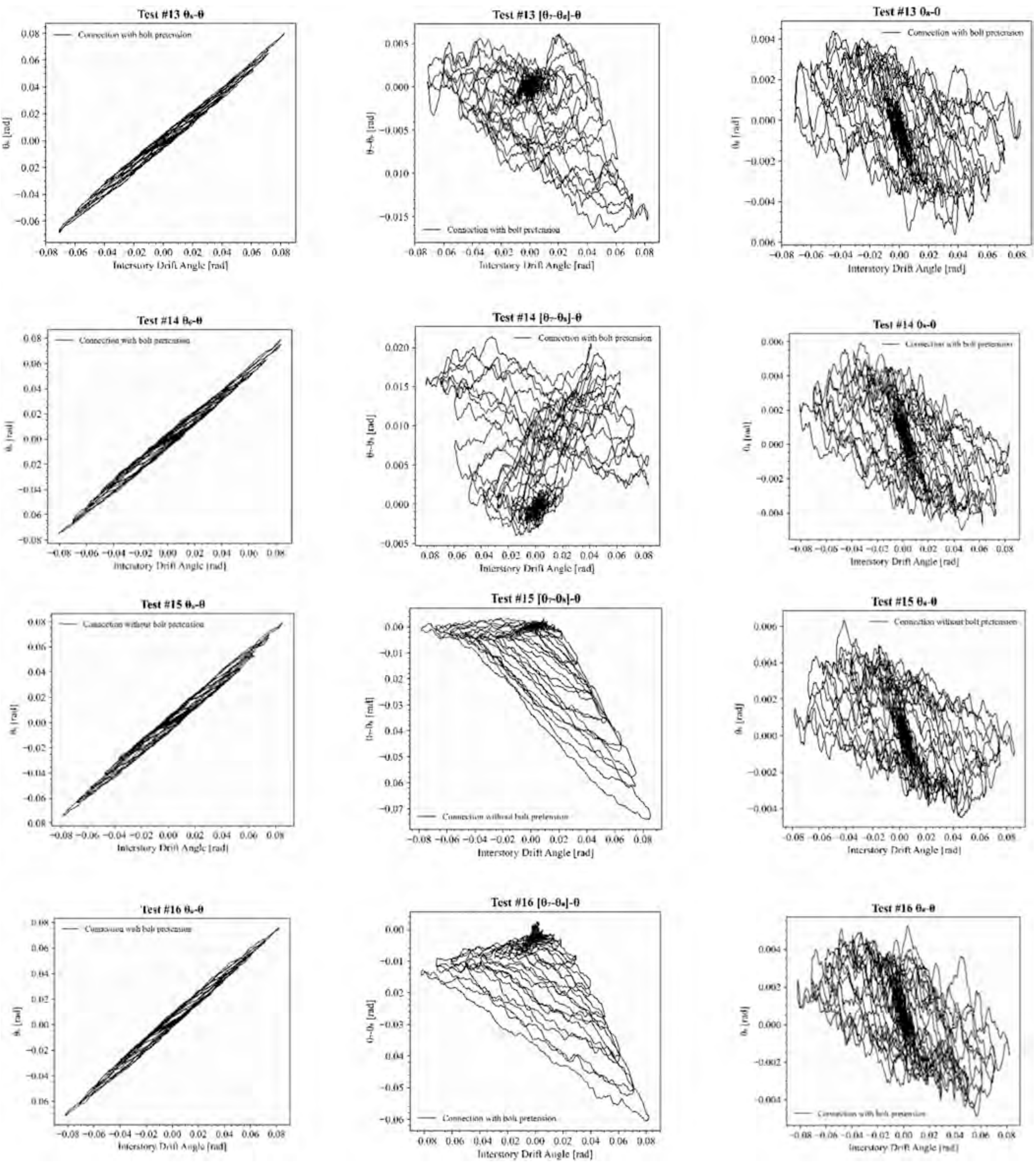

Fig. 8. (*continued*).

the specimens with lateral bolts, which shows that rotational capacity is lost in the component due to fracture in the weld.

On the other hand, the column shows a higher rotation capacity with a tendency to develop larger cycles unlike the beam near the connection and the L-connector. However, yielding, local buckling or fracture mechanisms in the column were not reported. Furthermore, for cycles greater than 2 % the column reached a local deformation of cross section similar to distortional buckling, however, the column was able of to recover its shape when the load direction changed.

4. Conclusions

The cyclic response of steel connections in bolted racks considering the influence of pretension on the behavior was studied through an experimental investigation. Sixteen full-scale tests were cyclically loaded. The evaluation was performed in terms of hysteretic behavior, failure mechanism, dissipated energy, secant stiffness and rotation in the joint components. The main conclusions obtained are described as follows:

1. The cyclic behavior exhibited by the beam-to-upright connections tested is characterized by a highly nonlinear behavior with hysteretic pinching and degradation of the secant stiffness once 4 % rotation is reached. Furthermore, the 80 % of the beam plastic moment (M_p) was not reached by the specimens, while the use of pretension in the bolts allowed some specimens to reach 75 % of the beam yield moment (M_y). Therefore, the steel design of the racks must take into account the stiffness and bending strength to reproduce the real system characteristics and deformations.
2. The failure mechanism was controlled by weld fracture once 4 % of the rotation was reached. The connections with front bolts reached higher levels of strength and rotation. The use of pretensioned bolts allowed the connections to develop rotation levels up to 17 % higher than connections without pretensioned bolts.
3. The accumulated dissipated energy showed that connections with front-bolts and bolts pretensioned achieved the higher level of dissipated energy. Additionally, the connections studied dissipate energy up to 6 % drift and from that level of rotation, the slope of the dissipation curve decreases, which is congruent with the level of damage reached in the weld for all connections. This phenomenon is due to the weld rupture between the beam connection and the L-connector.
4. A degradation of the secant stiffness without uniform pattern reached up to 60 % for 2 % rotation. While for 4 % the average secant stiffness can reach 30 % of the initial stiffness as residual stiffness in the system. This is due to weld fracture at 4 % rotation. Therefore, the stiffness degradation under cyclic loading of the system is an important aspect in the seismic design of racks.
5. The failure mechanism controlling the resistance limit states in the connections studied is weld fracture. This behavior limited the formation of ductile failure mechanisms in other components such as plastic hinges in the beams. Therefore, the design using bolted connections in racks is limited by good weld performance.

Data and code availability

The information corresponding to the results obtained in the reported trials belong to research of FONDEF IDEA ID22I10140 (ANID Research Project), with funds from the Chilean State, is part of a patent investigation and involves companies that finance the research project. Therefore, the information is considered confidential and cannot be shared.

Authorship Statement

Author Contributions: Conceptualization, Eduardo Nuñez; methodology, Eduardo Nuñez; software, Ramón Mata, Eduardo Nuñez and Matías Hernández; validation, Eduardo Nuñez, Marcelo Sanhueza; formal analysis, Eduardo Nuñez; investigation, Eduardo Nuñez; writing—original draft preparation, Eduardo Nuñez and Ramón Mata; writing—review and editing, Eduardo Nuñez; visualization, Eduardo Nuñez, Nelson Maureira and N é stor Guerrero; supervision, Eduardo Nuñez and Ramón Mata; project administration, Eduardo Nuñez.

All authors have read and agreed to the published version of the manuscript.

Funding

The research reported herein was possible thanks to the funding of FONDEF IDEA ID22I10140 (ANID Research Project), the Vice Rector's Office for Research and Graduate Studies and Postgraduate Direction of Universidad Católica de la S. Concepción for its scholarship.

CRediT authorship contribution statement

N é stor Guerrero: Writing – review & editing, Visualization, Data curation, Conceptualization. **Nelson Maureira:** Supervision, Funding acquisition. **Eduardo Nuñez:** Writing – review & editing, Writing – original draft, Visualization, Validation, Supervision, Software, Resources, Project administration, Methodology, Investigation, Funding acquisition, Formal analysis, Conceptualization. **Marcelo Sanhueza:** Software. **Ramón Mata:** Visualization, Validation, Supervision, Software. **Matías Hernández:** Software.

Declaration of Competing Interest

The authors declare that they have no known competing financial interests or personal relationships that could have appeared to influence the work reported in this paper.

Data availability

The data that has been used is confidential.

References

[1] Godley MHR. Plastic design of pallet rack beams. Thin-Walled Struct 1997;29(1–4):175–88.
[2] Aguirre C. Seismic behavior of rack structures. J Constr Steel Res 2005;61:607–24.
[3] Bajoria KM, Talikoti RS. Determination of flexibility of beam to column connectors used in thin walled cold-formed steel pallet racking systems. Thin-Walled Struct 2006;44:372–80.
[4] Sarawit AT, Pekoz T. Notional load method for industrial steel storage racks. Thin-Walled Struct 2006;44:1280–6.
[5] Bajoria KM, Sangle KK, Talicotti RS. Modal analysis of cold-formed pallet rack structures with semi-rigid connections. J Constr Steel Res 2010;66:428–41.
[6] Sangle KK, Bajoria KM, Talicotti RS. Elastic stability analysis of cold-formed pallet rack structures with semi-rigid connections. J Constr Steel Res 2012;71:245–62.
[7] Zhao X, Wang T, Chen Y, Sivakumaran KS. Flexural behavior of steel storage rack beam-to-upright connections. J Constr Steel Res 2014;99:161–75.
[8] Bernuzzi Claudio. European and United States approaches for steel storage pallet rack design: Part 1: Discussions and general comparisons." Thin-Walled Structures 2015;97:308–20.
[9] Bernuzzi Claudio, Draskovic Nikola, Simoncelli Marco. European and United States approaches for steel storage pallet rack design. Part 2: practical applications. Thin-walled Struct 2015;97:321–41.
[10] Yin L, Tang G, Zhang M, Wang B, Feng B. Monotonic and cyclic response of speed-lock connections with bolts in storage racks. Eng Struct 2016;116:40–55.
[11] Shah SNR, Sulong NR, Jumaat MZ, Shariati M. State-of-the-art review on the design and performance of steel pallet rack connections. Eng Fail Anal 2016;66:240–58.
[12] Zhao X, Dai L, Wang T, Sivakumaran KS, Chen Y. A theoretical model for the rotational stiffness of storage rack beam-to-upright connections. J Constr Steel Res 2017;133:269–81.
[13] Gusella F, Lavacchini G, Orlando M. Monotonic and cyclic tests on beam-column joints of industrial pallet racks. J Constr Steel Res 2018;140:92–107.
[14] Dai L, Zhao X, Rasmussen KJ. Flexural behaviour of steel storage rack beam-to-upright bolted connections. Thin-walled Struct 2018;124:202–17.
[15] Dai L, Zhao X, Rasmussen KJ. Cyclic performance of steel storage rack beam-to-upright bolted connections. J Constr Steel Res 2018;148:28–48.

[16] Gusella F, Arwade SR, Orlando M, Peterman KD. Influence of mechanical and geometric uncertainty on rack connection structural response. J Constr Steel Res 2019;153:343–55.

[17] Gusella F, Orlando M, Thiele K. Evaluation of rack connection mechanical properties by means of the Component Method. J Constr Steel Res 2018;149:207–24.

[18] Zhao X, Dai L, Rasmussen KJ. Hysteretic behaviour of steel storage rack beam-to-upright boltless connections. J Constr Steel Res 2018;144:81–105.

[19] Jovanović Đ, Žarković D, Vukobratović V, Brujić Z. Hysteresis model for beam-to-column connections of steel storage racks. Thin-Walled Struct 2019;142:189–204.

[20] Cardoso FS, Rasmussen KJ, Zhang H. System reliability-based criteria for the design of steel storage rack frames by advanced analysis: Part I–Statistical characterization of system strength. Thin-Walled Struct 2019;141:713–24.

[21] Cardoso FS, Zhang H, Rasmussen KJ. System reliability-based criteria for the design of steel storage rack frames by advanced analysis: part ii–reliability analysis and design applications. Thin-Walled Struct 2019;141:725–39.

[22] Galeotti C, Gusella F, Orlando M, Spinelli P. On the seismic response of steel storage pallet racks with selective addition of bolted joints (December). Structures, 34. Elsevier; 2021. p. 3806–17 (December).

[23] Bové O, López-Almansa F, Ferrer M, Roure F. Ductility improvement of adjustable pallet rack speed-lock connections: experimental study. J Constr Steel Res 2022;188:107015.

[24] Bové O, Ferrer M, López-Almansa F, Roure F. Numerical investigation on a seismic testing campaign on adjustable pallet rack speed-lock connections. Eng Struct 2022;252:113653.

[25] Liao H, Jiang SC, Wang YZ, Zhu S, Zhao X. Flexural behavior of clad rack beam-to-column bolted connections at high temperatures. J Constr Steel Res 2022;197:107506.

[26] López-Almansa F, Bové O, Casafont M, Ferrer M, Bonada J. State-of-the-art review on adjustable pallet racks testing for seismic design. Thin-Walled Struct 2022;181:110126.

[27] Romeo R, Puntel E, Pierobon S, Baldassino N. Component method applied to base plate connections of steel racks. J Constr Steel Res 2023;208:107999.

[28] Bernardi M, Baldassino N, Zandonini R, di Gioia A. Full-scale tests of industrial steel storage pallet racks (November). Structures, 57. Elsevier; 2023, 105128 (November).

[29] Yin L, Niu Y, Zheng Z, Tang G, Deng T, Li Z. Structural performance of speed-lock joints with split bolts in steel storage racks. J Constr Steel Res 2023;208:107991.

[30] ASTM A36/A36M. (2014). Standard specification for carbon structural steel. Philadelphia, PA, USA: Philadelphia American Society for Testing and Materials.

[31] ASTM A325/A325M. (2014). Standard Specification for Structural Bolts, Steel, Heat Treated, 120/105ksi Minimum Tensile Strength. Philadelphia, PA, USA: Philadelphia American Society for Testing and Materials.

[32] ANSI/AISC 360–16. Chicago, IL, USA: American Institute of Steel Construction; 2016.

[33] ANSI/AISC 341-16. Chicago, IL, USA: American Institute of Steel Construction; 2016.